Role of Tyr$^{356(7.43)}$ and Ser$^{190(4.57)}$ in Antagonist Binding in the Rat β_1-Adrenergic Receptor

Linda A. Rezmann-Vitti,[†] Tracy L. Nero,[†] Graham P. Jackman,[†] Curtis A. Machida,[‡] Brian J. Duke,[§] William J. Louis,[†] and Simon N. S. Louis*,[†]

Department of Medicine, Austin Health, Clinical Pharmacology and Therapeutics Unit, The University of Melbourne, Heidelberg, 3084, Victoria, Australia, Department of Integrative Biosciences, School of Dentistry, Oregon Health and Science University, Portland, Oregon 97239, and Department of Medicinal Chemistry, Victorian College of Pharmacy, Monash University, Parkville, 3052, Victoria, Australia

Received July 1, 2005

Site-directed mutagenesis and photoaffinity labeling experiments suggest the existence of at least two distinct binding orientations for aryloxypropanolamine competitive antagonists in the β-adrenergic receptor (β-AR), one where the aryloxy moiety is located near transmembrane α-helix 7 (tm 7) and another where it is near tm 5. To explore a hydrophobic pocket involving tms 1, 2, 3, and 7 for potential aryloxy interaction sites, we selected Tyr$^{356(7.43)}$ and Trp$^{134(3.28)}$ in the rat β_1-AR for site-directed mutagenesis studies. Ser$^{190(4.57)}$ was also investigated, as the equivalent residues are known antagonist interaction sites in the muscarinic M_1 and the dopamine D_2 receptors. Binding affinities (pK_i) of a series of structurally diverse aryloxypropanolamine competitive antagonists were determined for wild type and Y356A, Y356F, W134A, and S190A mutant rat β_1-ARs stably expressed in Chinese hamster ovary cells. To visualize possible antagonist/receptor interactions, the compounds were docked into a three-dimensional model of the wild-type rat β_1-AR. The results indicate that Tyr$^{356(7.43)}$ is an important aromatic interaction site for five of the eight competitive antagonists studied, whereas none of the compounds appeared to interact directly with Trp$^{134(3.28)}$. Only two of the competitive antagonists interacted with Ser$^{190(4.57)}$ on tm 4. Overall, the results extend our understanding of how β_1-AR competitive antagonists bind to the hydrophobic pocket involving tms 1, 2, 3, and 7; highlight the importance of Tyr$^{356(7.43)}$ in this binding pocket; and demonstrate the involvement of tm 4 in competitive antagonist binding.

Introduction

Agonists must make specific interactions with a receptor to induce precise conformational changes that result in receptor activation, whereas competitive antagonists need only bind to the receptor in a way that interferes with agonist binding.[1−4] In contrast to agonists,[2,5−15] few β-adrenergic receptor (β-AR[a]) residues involved in competitive antagonist binding have been identified. In the β-AR it is generally accepted[6] that the interaction site for the competitive antagonist amine nitrogen is Asp$^{(3.32)}$, and for the rat β_1-AR this residue is Asp$^{138(3.32)}$ (using the amino acid residue numbering system devised by Ballesteros and Weinstein[15]). Many aryloxypropanolamine competitive β-AR antagonists also bind with high affinity to 5-hydroxytryptamine$_{1A}$ receptors (5-HT$_{1A}$Rs) and 5-HT$_{1B}$Rs,[16−22] and site-directed mutagenesis studies of β_2-ARs, 5-HT$_{1A}$Rs, and 5-HT$_{1B}$Rs have identified Asn$^{(7.39)}$ as an interaction site for the aryloxy oxygen and/or the β-hydroxyl group of propranolol (**1**), alprenolol (**2**), and pindolol (**3**) (Figure 1).[12,16−20,22−24] In the rat β_1-AR this residue is Asn$^{352(7.39)}$. However, the para-substituted phenoxypropanolamines practolol (**4**) and atenolol (**5**) and the aryletha-nolamine sotalol (**6**) (Figure 1) do not appear to interact with Asn$^{(7.39)}$, as their binding affinities are unaffected by mutation of this residue.[19,21,22]

When a competitive antagonist interacts with the rat β_1-AR, while maintaining the interactions described above for Asp$^{138(3.32)}$ and Asn$^{352(7.39)}$, the aryloxy ring is located in a hydrophobic pocket defined by residues in transmembrane α-helices (tms) 1, 2, 3, and 7 (refer to Figure 2). Two aromatic residues in this pocket, Tyr$^{356(7.43)}$ and Trp$^{134(3.28)}$, are ideally located to interact with the antagonist aryloxy ring. In a preliminary communication we reported the binding affinities of cyanopindolol (**7**) and [^{125}I]-iodocyanopindolol (^{125}I-CYP, **8**) for the Y356A and Y356F mutant rat β_1-ARs.[25] We observed a >5000-fold decrease in the binding affinity (pK_i) of compound **7** for the Y356A mutant receptor, when compared to the wild-type (WT) rat β_1-AR. In contrast, the Y356F mutation maintained compound **7** binding at WT levels. The data suggested that compound **7** interacted directly with Tyr$^{356(7.43)}$, via predominantly aromatic interactions.[25] Like compound **7**, the Y356F mutant receptor maintained the binding affinity of the structural analogue **8** at WT levels. However, unlike compound **7**, only a 3-fold decrease in the binding affinity of compound **8** was observed for the Y356A mutant rat β_1-AR. Our initial interpretation of the data for compound **8** was that Tyr$^{356(7.43)}$ was not an interaction site for this competitive antagonist and that compound **8** bound to the WT β_1-AR in a different orientation to that adopted by compound **7**.[25]

The purpose of the present work was to further explore competitive antagonist binding orientations of a range of structurally diverse aryloxypropanolamines by (i) examining their interactions with the hydrophobic pocket defined by residues in tms 1, 2, 3, and 7, specifically interactions with Tyr$^{356(7.43)}$ and Trp$^{134(3.28)}$, and (ii) determine whether Ser$^{190(4.57)}$ is involved in

* To whom correspondence should be addressed. Tel: +61-3-94965486. Fax: +61-3-94593510. E-mail: simonnsl@unimelb.edu.au.
[†] The University of Melbourne.
[‡] Oregon Health and Science University.
[§] Monash University.

[a] Abbreviations: β-ARs, β-adrenergic receptors; 5HTRs, 5-hydroxytryptamine receptors; tm, transmembrane; CHO, Chinese hamster ovary; WT, wild-type; G418, geneticin; BSA, bovine serum albumin; K_d, dissociation constant; K_i, inhibition constant; (*S*)-D140, (*S*)-(−)-1-(4-ethoxyethoxyphenyl)-2-hydroxy-3-(3,4-dimethoxyphenyl)ethylaminopropane; LK204-545, (±)-1-(2-(3-cyano-4-(2-cyclopropylmethoxyethoxy)phenoxy)-2-hydroxypropylamino)ethyl-3-(4-hydroxyphenyl)urea; CGP20712A, (±)-2-hydroxy-5-[2-[[2-hydroxy-3-[4-[1-methyl-4-(trifluoromethyl)-1*H*-imidazol-2-yl]phenoxy]propyl]amino]ethoxy]benzamide; ^{125}I-CYP, [^{125}I]iodocyanopindolol; ^{125}I-AmF, [^{125}I]iodoaminoflisoprolol.

10.1021/jm050624l CCC: $33.50
Published on Web 05/12/2006

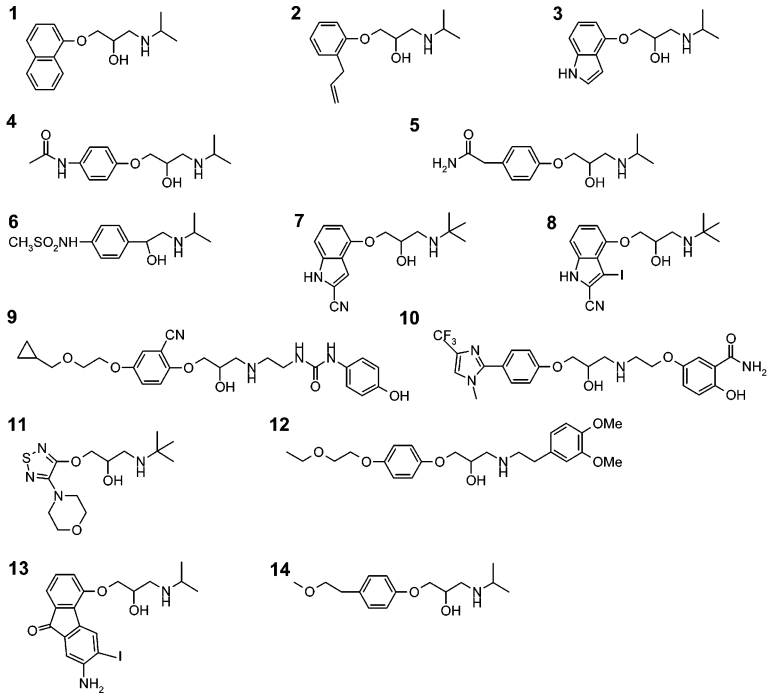

Figure 1. Chemical structures of propranolol (**1**), alprenolol (**2**), pindolol (**3**), practolol (**4**), atenolol (**5**), sotalol (**6**), cyanopindolol (**7**), ^{125}I-CYP (**8**), LK204-545 (**9**), CGP20712A (**10**), timolol (**11**), D140 (**12**), ^{125}I-AmF (**13**), and metoprolol (**14**).

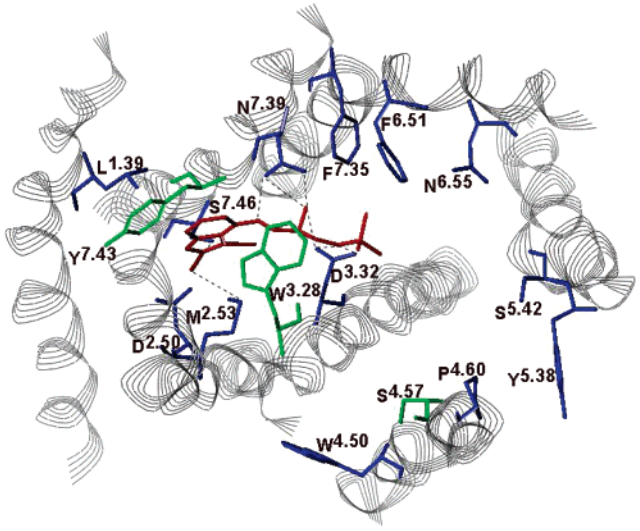

Figure 2. Putative (*S*)-**8** (red) interactions with the WT rat β_1-AR model. In this binding orientation both the amine nitrogen and β-hydroxyl group can interact with Asp$^{138(3.32)}$, while Asn$^{352(7.39)}$ hydrogen bonds with both the aryloxy oxygen and the β-hydroxyl group of (*S*)-**8**. The aryloxy moiety is located in the hydrophobic pocket defined by Leu$^{65(1.39)}$, Met$^{107(2.53)}$, Val$^{111(2.57)}$, Val$^{112(2.58)}$, Gly$^{115(2.61)}$, Trp$^{134(3.28)}$, Asn$^{352(7.39)}$, Trp$^{353(7.40)}$, and Tyr$^{356(7.43)}$ and forms edge-to-face $\pi-\pi$ interactions with Trp$^{353(7.40)}$ and Tyr$^{356(7.43)}$. The cyano group can interact with both Met$^{107(2.53)}$ and Ser$^{359(7.46)}$. The iodine is located in a pocket formed by Met$^{107(2.53)}$, Val$^{111(2.57)}$, Asp$^{138(3.32)}$, Cys$^{141(3.35)}$, Trp$^{326(6.48)}$, Gly$^{355(7.42)}$, and Ser$^{359(7.46)}$. The *tert*-butyl group is surrounded by Trp$^{134(3.28)}$, Thr$^{135(3.29)}$, Asp$^{138(3.32)}$, Trp$^{326(6.48)}$, Phe$^{329(6.51)}$, and Phe$^{348(7.35)}$. The tm regions are shown as gray ribbons. The three residues mutated in this study are shown in green. Putative hydrogen bonds are displayed as dashed lines. Hydrogen atoms are not displayed. The view is an extracellular one, looking down through the ligand binding site. For simplicity, the residues are labeled using only the one letter amino acid code, with the universal residue number as a superscript.

competitive antagonist binding in the rat β_1-AR. It has been previously reported that Ser$^{(4.57)}$ in the human β_2-AR is not important for compound **8** binding.[11] However, in the rat muscarinic M_1 receptor and the human dopamine D_2 receptor the equivalent residue to Ser$^{190(4.57)}$ has been shown to play a role in antagonist binding,[26,27] and we now confirm that this residue also plays a role in the binding of competitive antagonists to the rat β_1-AR.

Ser$^{(4.57)}$ and Tyr$^{(7.43)}$ are conserved across the adrenergic receptor family, while at position 3.28 the residue is either Trp or Tyr (GPCRDB[28] sequence alignment, March 2005 release 9.0, available at www.gpcr.org/7tm/). We have specifically chosen to study competitive β_1-AR antagonists because of their clinical importance and the availability of a diverse range of potent and selective compounds.[29−31] The previously described Tyr$^{356(7.43)}$ mutants,[25] Y356A and Y356F, were used in this study; Trp$^{134(3.28)}$ was mutated to Ala (W134A), removing the potential for this residue to participate in both aromatic and hydrogen-bond interactions, and Ser$^{190(4.57)}$ was mutated to Ala (S190A), removing the potential for hydrogen bonding. The binding affinities (pK_i) of seven structurally diverse competitive antagonists for the Y356A, Y356F, W134A, and S190A mutant receptors are reported and compared to their pK_i values for the WT rat β_1-AR. A three-dimensional model of the WT rat β_1-AR,[14,25] based on the bovine rhodopsin crystal structure,[32] was used to aid in the interpretation of the experimental results and visualize possible antagonist interactions with the three mutated residues. The results expand our understanding of the antagonist aryloxy ring interactions with Tyr$^{356(7.43)}$ and confirm that Ser$^{190(4.57)}$ also plays a role in the binding of some competitive antagonists. However, the results have also required us to revise our initial hypothesis for the binding orientation of compound **8**.[25] For this reason we have also included the pK_i and pK_d data for compounds **7** and **8**, respectively, for the Y356A and Y356F mutant receptors previously published in a preliminary communication (ref 25 and Table 1).

Results

^{125}I-CYP (Compound 8) Radioligand Binding. Binding results for the competitive β-AR antagonists are presented in Table 1. In saturation-binding studies, the radioligand ^{125}I-CYP

Table 1. Competitive Antagonist Affinities for the WT and Mutant Rat β_1-ARs

		WT	Y356F	Y356A	W134A	S190A
1	propranolol	8.5 ± 0.03	7.5 ± 0.1 (9)[a]	6.7 ± 0.05 (55)[a]	8.0 ± 0.1 (3)[a]	7.4 ± 0.1 (10)[a]
7	cyanopindolol	10.3 ± 0.01	10.4 ± 0.04	6.5 ± 0.04 (6310)[a]	9.9 ± 0.1 (3)[b]	9.5 ± 0.2 (6)[a]
8	125I-CYP[c]	10.2 ± 0.02	10.1 ± 0.1	9.5 ± 0.1 (5)[a]	10.2 ± 0.03	10.2 ± 0.03
9	LK204-545	8.1 ± 0.1	7.1 ± 0.1(10)[a]	4.1 ± 0.1 (10471)[a]	7.2 ± 0.01 (7)[a]	7.0 ± 0.1 (14)[a]
10	CGP20712A	8.9 ± 0.2	8.7 ± 0.1 (2)	5.0 ± 0.04 (10000)[a]	8.1 ± 0.1(7)[a]	6.1 ± 0.04 (690)[a]
11	timolol	8.5 ± 0.1	7.8 ± 0.1 (5)[b]	6.2 ± 0.2 (190)[a]	8.1 ± 0.02 (3)	7.5 ± 0.1 (9)[a]
(*S*)-**12**	(*S*)-D140	7.3 ± 0.1	7.0 ± 0.1 (3)[b]	6.1 ± 0.1 (15)[a]	7.1 ± 0.1 (2)	4.9 ± 0.1 (275)[a]
14	metoprolol	6.4 ± 0.01	5.6 ± 0.1 (6)[a]	5.3 ± 0.2 (12)[a]	6.2 ± 0.1 (2)	5.6 ± 0.1 (6)[a]
B_{max}[d]		417 ± 132	256 ± 30	689 ± 91	570 ± 70	379 ± 5

[a] $p < 0.01$. [b] $p < 0.05$ vs WT. [c] pK_d from saturation studies as described in the Experimental Section. [d] Receptor binding density (in fmol/mg) of compound **8**. Antagonist pK_i values were determined in competition binding as described in the Experimental Section. Values in parentheses represent the fold change in affinity relative to the WT receptor. Data are reported as the mean ± SEM of three to five independent experiments performed in triplicate.

(compound **8**) bound to the Y356A, Y356F, W134A, and S190A mutant receptors with similar affinity and density (B_{max}) to the WT rat β_1-AR, except that the pK_d value for the Y356A mutant was slightly lower than for WT (9.5 ± 0.1 vs 10.2 ± 0.02, $p < 0.01$).

Competition Analysis. The binding curves for all competitive antagonists and receptors were consistent with a single binding site ($n_H = 0.89-1$). However, the very low affinity of (±)-1-(2-(3-cyano-4-(2-cyclopropylmethoxyethoxy)phenoxy)-2-hydroxypropylamino)-ethyl-3-(4-hydroxyphenyl)urea (LK204-545, **9**) for the Y356A mutant prevented a preferred binding site from being statistically determined.

The para-substituted β_1-selective antagonists (±)-2-hydroxy-5-[2-[[2-hydroxy-3-[4-[1-methyl-4-(trifluoromethyl)-1*H*-imidazol-2-yl]phenoxy]propyl]amino]ethoxy]benzamide (CGP20712A, **10**) and compound **9**, like the nonselective antagonist **7**, showed dramatic and significant reductions in binding affinity (>10 000-fold, $p < 0.01$) for the Y356A mutant when compared to the WT β_1-AR (Table 1). In contrast to compound **7**, the radioiodinated analogue **8** had only a small reduction (5-fold) in pK_d for this mutant (Table 1). As with compound **7**, the Y356F mutation fully restored the affinity of compound **10** to that of WT receptor levels, and the reduction in binding affinity for compound **9** was now only 10-fold. Compound **1** and timolol (**11**) also displayed significantly reduced affinities (55- and 190-fold respectively, $p < 0.01$) for the Y356A mutant receptor, while the more conservative Y356F substitution maintained binding affinities for these two antagonists close to WT levels (9 and 5-fold reduction in binding affinity respectively).

An involvement of tm 4 in binding two of the competitive antagonists was also demonstrated. S190A mutant receptors displayed reduced affinity (275- and 690-fold, respectively) for (*S*)-(−)-1-(4-ethoxyethoxyphenyl)-2-hydroxy-3-(3,4-dimethoxyphenyl)ethylaminopropane [(*S*)-D140, (*S*)-**12**] and compound **10** when compared to the WT rat β_1-AR. In comparison, the reduction in affinity was ≤14-fold for the other antagonists examined. The W134A mutation produced only small reductions in binding affinity (≤7-fold) for all the competitive antagonists studied (Table 1).

Visualization of Putative Antagonist Interactions with Tyr$^{356(7.43)}$ and Ser$^{190(4.57)}$ in the WT Rat β_1-AR Model. Interaction with Asp$^{138(3.32)}$ was deemed to be essential when docking competitive antagonists into the rat β_1-AR model. The antagonists are very flexible and can readily adopt a variety of feasible conformations. A fully extended low-energy conformation was used as the starting point in the manual docking studies, and the antagonist torsion angles were then varied in order to maximize the interactions between the antagonist and β_1-AR ligand binding site. The examples below describe antagonist conformations that maximize the interactions with the ligand binding site and are consistent with the binding affinity data presented in Table 1.

(*S*)-^{125}I-CYP [(*S*)-8] and (*S*)-Timolol [(*S*)-11]. Mutation of Tyr$^{356(7.43)}$ had only a small effect on the binding of compound **8** (5-fold reduction compared to WT receptor, Table 1 and ref 25), indicating that this residue is not an important interaction site for the aryloxy moiety. Initial docking studies showed that the (*S*)-**8** aryloxy moiety can be accommodated in the hydrophobic pocket defined by residues in tms 1, 2, 3, and 7; however, the (*S*)-**8** conformations previously examined were energetically unstable (i.e., not stationary points).[25] On the basis of these initial docking studies, we proposed that the aryloxy moiety of (*S*)-**8** did not bind in the hydrophobic pocket located near tms 1, 2, 3, and 7.[25] One of the proposed alternative binding pockets for the (*S*)-**8** aryloxy moiety is located near tms 6 and 7, with the aryloxy interacting with Phe$^{329(6.51)}$, Asn$^{333(6.55)}$, and Phe$^{348(7.35)}$; both the (*S*)-**8** β-hydroxyl and amine nitrogen interacting with Asp$^{138(3.32)}$ and Asn$^{352(7.39)}$; and the *tert*-butyl group surrounded by Val$^{111(2.57)}$, Trp$^{134(3.28)}$, Thr$^{135(3.29)}$, Asp$^{138(3.32)}$, Asn$^{352(7.39)}$ and Trp$^{353(7.40)}$.[25] However, the binding affinity (pK_i) data for compound **11** (Table 1) indicated that our original hypothesis for (*S*)-**8** binding had to be revised.

Compound **11** exhibited a 190-fold loss in binding affinity for the Y356A mutant receptor, compared to WT, whereas only a 5-fold decrease in affinity was observed for the Y356F mutation (Table 1). These results suggest that compound **11** interacts with Tyr$^{356(7.43)}$ via predominantly aromatic interactions. The small reductions in pK_i for both the W134A and S190A mutant receptors, compared to WT, suggests that compound **11** does not form any significant interactions with either of these residues. (*S*)-**11** was docked into the WT rat β_1-AR model with the aryloxy moiety interacting with Tyr$^{356(7.43)}$ and both the β-hydroxyl and amine nitrogen interacting with Asp$^{138(3.32)}$. When binding in this orientation, the morpholino ring is located in a pocket defined by Met$^{107(2.53)}$, Val$^{111(2.57)}$, Asp$^{138(3.32)}$, Cys$^{141(3.35)}$, Trp$^{326(6.48)}$, Tyr$^{356(7.43)}$, and Ser$^{359(7.46)}$. The morpholino ring oxygen is able to hydrogen bond to both Met$^{107(2.53)}$ and Cys$^{141(3.35)}$, while the aryloxy oxygen interacts with Asn$^{352(7.39)}$. The aryloxy ring is located in a hydrophobic pocket defined by Leu$^{65(1.39)}$, Met$^{107(2.53)}$, Val$^{111(2.57)}$, Val$^{112(2.58)}$, Gly$^{115(2.61)}$, Trp$^{134(3.28)}$, Asn$^{352(7.39)}$, Trp$^{353(7.40)}$, and Tyr$^{356(7.43)}$ and makes edge-to-face $\pi-\pi$ interactions with Trp$^{353(7.40)}$ and Tyr$^{356(7.43)}$. The (*S*)-**11** *tert*-butyl group is surrounded by Trp$^{134(3.28)}$, Thr$^{135(3.29)}$, Asp$^{138(3.32)}$, Phe$^{329(6.51)}$, and Phe$^{348(7.35)}$. When docked in this orientation, (*S*)-**11** makes no significant interactions with either Trp$^{134(3.28)}$ or Ser$^{190(4.57)}$. Flexible superimposition indicated that (*S*)-**8** could bind in a similar orientation to the WT rat β_1-AR, where the iodine is located in the same pocket as that occupied by the (*S*)-**11** morpholino ring. However, this requires an explanation for the small effect of the Y356A mutation on the pK_d of (*S*)-**8.**

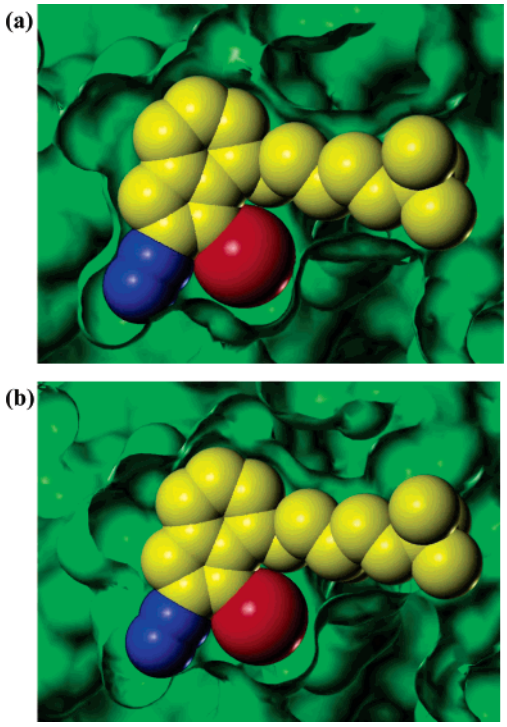

Figure 3. Connolly surface of the ligand binding pockets for the (a) WT and (b) Y356A rat β_1-AR. (*S*)-**8** (CPK representation) is shown interacting with the aryloxy moiety located in the tms 1, 2, 3, and 7 hydrophobic pocket (i.e., the same orientation as that depicted in Figure 2). The binding of both the cyano group (blue) and the iodine (red) in the pockets shown in parts a and b may serve to anchor the antagonist in the receptor and contribute significantly to the binding affinity.

Reexamination of the (*S*)-**8** conformations used previously in docking studies indicated that the conformational space of this compound had not been sufficiently sampled. We have now repeated the (*S*)-**8** docking studies and found that stable, low-energy conformations of (*S*)-**8** can adopt an orientation analogous to that described above for (*S*)-**11**. When binding in this orientation (Figure 2) the aryloxy moiety of (*S*)-**8** is located in the tms 1, 2, 3, and 7 hydrophobic pocket (defined by residues Leu$^{65(1.39)}$, Met$^{107(2.53)}$, Val$^{111(2.57)}$, Val$^{112(2.58)}$, Gly$^{115(2.61)}$, Trp$^{134(3.28)}$, Asn$^{352(7.39)}$, Trp$^{353(7.40)}$, and Tyr$^{356(7.43)}$) and makes edge-to-face $\pi-\pi$ interactions with Trp$^{353(7.40)}$ and Tyr$^{356(7.43)}$. The cyano group can interact with both Met$^{107(2.53)}$ and Ser$^{359(7.46)}$. The iodine is located in a pocket defined by Met$^{107(2.53)}$, Val$^{111(2.57)}$, Asp$^{138(3.32)}$, Cys$^{141(3.35)}$, Trp$^{326(6.48)}$, Gly$^{355(7.42)}$, and Ser$^{359(7.46)}$ and may interact with these residues via steric and/or noncovalent interactions. The aryloxy oxygen interacts with Asn$^{352(7.39)}$ and the β-hydroxyl can hydrogen bond to both Asp$^{138(3.32)}$ and Asn$^{352(7.39)}$. The (*S*)-**8** amine nitrogen interacts with Asp$^{138(3.32)}$, and the *tert*-butyl group is surrounded by Trp$^{134(3.28)}$, Thr$^{135(3.29)}$, Asp$^{138(3.32)}$, Trp$^{326(6.48)}$, Phe$^{329(6.51)}$, and Phe$^{348(7.35)}$. The binding affinities for the WT and mutant rat β_1-ARs (Table 1) indicate that interactions with Trp$^{134(3.28)}$, Ser$^{190(4.57)}$, or Tyr$^{356(7.43)}$ are not essential for (*S*)-**8** binding. One interpretation of the data presented in Table 1 is that the aryloxy moiety of (*S*)-**8** does not bind in the manner depicted in Figure 2 (i.e., does not bind in the hydrophobic pocket formed by residues in tms 1, 2, 3, and 7), and this was our original hypothesis for (*S*)-**8** binding.[25] However, an alternative hypothesis became apparent when we examined the Connolly surface of the ligand binding pockets of both the WT and Y356A β_1-AR models (Figure 3). When (*S*)-**8** adopts the orientation depicted in Figure 2, the bulky iodine fits snugly into the binding pocket defined by Met$^{107(2.53)}$, Val$^{111(2.57)}$, Asp$^{138(3.32)}$, Cys$^{141(3.35)}$, Trp$^{326(6.48)}$, Gly$^{355(7.42)}$, and Ser$^{359(7.46)}$ in the WT receptor (Figure 3a). A similar scenario also exists in the Y356A mutant (Figure 3b). It is plausible that the iodine acts as an anchor, allowing the compound to maximize the interactions it makes with the receptor and that replacement of Tyr$^{356(7.43)}$ has little effect on this process.

(*S*)-Cyanopindolol [(*S*)-7] and (*S*)-Propranolol [(*S*)-1]. The data reported here for the W134A and S190A mutant receptors, together with the data for the Y356F and Y356A mutants reported in the preliminary communication (Table 1 and ref 25), suggest that (*S*)-**7** forms significant aromatic interactions with Tyr$^{356(7.43)}$ but does not interact with either Trp$^{134(3.28)}$ or Ser$^{190(4.57)}$. The importance of the interaction with Tyr$^{356(7.43)}$ contrasts with the results for compound **8**. This suggests that the iodine atom of (*S*)-**8** may play an important role in orientating the antagonist within the ligand binding pocket. When docking (*S*)-**7** into the WT rat β_1-AR, in a manner analogous to that shown in Figure 2 for (*S*)-**8**, the aryloxy moiety of (*S*)-**7** is located in a hydrophobic pocket defined by Leu$^{65(1.39)}$, Met$^{107(2.53)}$, Val$^{111(2.57)}$, Val$^{112(2.58)}$, Gly$^{115(2.61)}$, Trp$^{134(3.28)}$, Asn$^{352(7.39)}$, Trp$^{353(7.40)}$, and Tyr$^{356(7.43)}$ and makes edge-to-face $\pi-\pi$ interactions with Trp$^{353(7.40)}$ and Tyr$^{356(7.43)}$. When binding in this aryloxy moiety orientation, Asn$^{352(7.39)}$ and Asp$^{138(3.32)}$ can interact with both the (*S*)-**7** amine nitrogen and the β-hydroxyl. Asn$^{352(7.39)}$ is also able to hydrogen bond to the (*S*)-**7** aryloxy oxygen. The (*S*)-**7** *tert*-butyl group is surrounded by Trp$^{134(3.28)}$, Thr$^{135(3.29)}$, Val$^{139(3.33)}$, Phe$^{329(6.51)}$, and Phe$^{348(7.35)}$ and the cyano group can hydrogen bond to Ser$^{359(7.46)}$. When docked in this orientation, (*S*)-**7** is unable to interact with either Trp$^{134(3.28)}$ or Ser$^{190(4.57)}$.

When interacting with Asp$^{138(3.32)}$, Asn$^{352(7.39)}$, and Tyr$^{356(7.43)}$ (*S*)-**1** can only adopt a binding orientation similar to that of (*S*)-**7**, (*S*)-**8**, and (*S*)-**11** and does not interact with either Trp$^{134(3.28)}$ or Ser$^{190(4.57)}$ (the location of (*S*)-**1** is analogous to that of (*S*)-**8** in Figure 2).

The competitive antagonists **9**, **10**, and **12** are examples of para-substituted phenoxypropanolamines containing large amine substituents, and they are of particular interest because of their high degree of β_1-AR specificity.[29−31]

(*S*)-CGP20712A [(*S*)-10]. Compound **10** displayed large reductions in affinity, compared to WT, for the Y356A (10 000-fold) and S190A (690-fold) mutations, highlighting the importance of these two residues in maintaining the antagonist in an optimum binding orientation (i.e., maximizing the interactions with the receptor). Binding was maintained at WT levels by the Y356F mutant (Table 1). Figure 4 illustrates how (*S*)-**10** can simultaneously interact with Tyr$^{356(7.43)}$ (aromatic interaction), Ser$^{190(4.57)}$ (hydrogen bond), and Asp$^{138(3.32)}$ (hydrogen bond/salt bridge) in the rat β_1-AR when the aryloxy moiety is located in the hydrophobic pocket formed by tms 1, 2, 3, and 7 (defined by residues Leu$^{65(1.39)}$, Met$^{107(2.53)}$, Val$^{111(2.57)}$, Val$^{112(2.58)}$, Gly$^{115(2.61)}$, Trp$^{134(3.28)}$, Asn$^{352(7.39)}$, Trp$^{353(7.40)}$, and Tyr$^{356(7.43)}$). In this binding orientation Tyr$^{356(7.43)}$ and Trp$^{353(7.40)}$, but not Trp$^{134(3.28)}$, form edge-to-face $\pi-\pi$ interactions with the bi-ring aryloxy moiety of (*S*)-**10**. The amine substituent phenyl ring is located in a pocket defined by residues in tms 3, 4, and 5 (i.e., Thr$^{135(3.29)}$, Ser$^{136(3.30)}$, Val$^{139(3.33)}$, Val$^{189(4.56)}$, Ser$^{190(4.57)}$, Pro$^{193(4.60)}$, Ser$^{228(5.42)}$, and Tyr$^{224(5.38)}$). The distance between the centroids of the amine substituent phenyl ring and the phenyl ring of Tyr$^{224(5.38)}$ is approximately 7.8 Å, making direct aromatic interactions between these two ring systems possible but unlikely. The *m*-amide functional group of the (*S*)-**10** amine substituent is able to interact with Ser$^{190(4.57)}$ via a hydrogen bond, while the *p*-hydroxyl group interacts with Ser$^{228(5.42)}$. Asp$^{138(3.32)}$ interacts with both the amine nitrogen and the

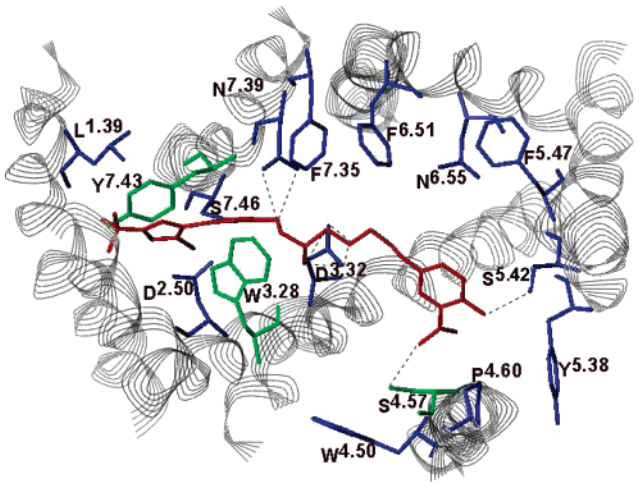

Figure 4. (*S*)-**10** (red) interactions with the WT rat β_1-AR model. In this binding orientation the *m*-amide of the amine substituent interacts with Ser$^{190(4.57)}$ and the *p*-hydroxyl binds to Ser$^{228(5.42)}$. The amine substituent phenyl ring is surrounded by Thr$^{135(3.29)}$, Val$^{189(4.56)}$, Pro$^{193(4.60)}$, Val$^{139(3.33)}$, Ser$^{136(3.30)}$, Ser$^{190(4.57)}$, and Tyr$^{224(5.38)}$. Both the (*S*)-**10** β-hydroxyl group and amine nitrogen are able to interact with Asp$^{138(3.32)}$. Asn$^{352(7.39)}$ hydrogen bonds to the aryloxy oxygen of (*S*)-**10**. The bi-ring aryloxy moiety of (*S*)-**10** sits in the hydrophobic pocket defined by Leu$^{65(1.39)}$, Met$^{107(2.53)}$, Val$^{111(2.57)}$, Val$^{112(2.58)}$, Gly$^{115(2.61)}$, Trp$^{134(3.28)}$, Asn$^{352(7.39)}$, Trp$^{353(7.40)}$, and Tyr$^{356(7.43)}$ and forms edge-to-face $\pi-\pi$ interactions with Trp$^{353(7.40)}$ and Tyr$^{356(7.43)}$. The color scheme and representations are the same as for Figure 2.

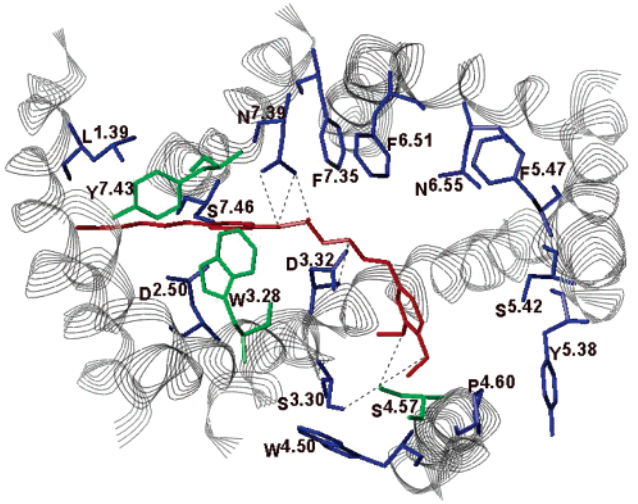

Figure 5. Putative (*S*)-**12** (red) interactions with the WT rat β_1-AR model. The amine substituent *m*-methoxy oxygen interacts with Ser$^{190(4.57)}$ and the *p*-methoxy oxygen interacts with Ser$^{136(3.30)}$ via hydrogen bonds. The amine substituent phenyl ring is surrounded by Val$^{139(3.31)}$, Pro$^{193(4.60)}$, Ser$^{136(3.30)}$, Leu$^{140(3.34)}$, Val$^{137(3.31)}$, Asp$^{138(3.32)}$, Thr$^{135(3.29)}$, and Ile$^{194(4.61)}$. Asn$^{352(7.39)}$ interacts with both the aryloxy oxygen and the β-hydroxyl group of (*S*)-**12**. The amine nitrogen interacts with Asp$^{138(3.32)}$. The aryloxy ring sits at the entrance to the hydrophobic binding pocket defined by Leu$^{65(1.39)}$, Met$^{107(2.53)}$, Val$^{111(2.57)}$, Val$^{112(2.58)}$, Gly$^{115(2.61)}$, Trp$^{134(3.28)}$, Asn$^{352(7.39)}$, Trp$^{353(7.40)}$, and Tyr$^{356(7.43)}$ and makes edge-to-face $\pi-\pi$ interactions with Trp$^{353(7.40)}$. The aryloxy para-substituent extends into this hydrophobic pocket and the ether oxygen is able to interact with the backbone carbonyl group of both Val$^{112(2.58)}$ and Gly$^{115(2.61)}$. The color scheme and representations are the same as for Figure 2.

β-hydroxyl group of the antagonist. In this orientation Asn$^{352(7.39)}$ interacts with the aryloxy oxygen. When viewed as in Figure 4, (*S*)-**10** occupies the entire width of the receptor channel and may physically prevent agonist molecules from accessing the agonist binding site (the agonist binding site is described in ref 15). The physical size of (*S*)-**10** also restricts the depth at which the antagonist can bind in the receptor channel and it is located closer to the β_1-AR extracellular surface than the agonist binding site (which includes Phe$^{233(5.47)}$, Phe$^{329(6.51)}$, and Phe$^{330(6.52)}$). The more extracellular location of (*S*)-**10** is consistent with the view that competitive antagonists generally bind higher in the receptor channel, preventing the agonist from gaining access to the binding site.[33−35]

When (*S*)-**10** is docked into the ligand binding site with the aryloxy moiety interacting with Tyr$^{224(5.38)}$ in tm 5, in a manner consistent with [^{125}I]iodoaminoflisoprolol (^{125}I-AmF, **13**) binding in the β_2-AR as described by Wu et al.,[33] the interactions with Tyr$^{356(7.43)}$, Asn$^{352(7.39)}$, and Asp$^{138(3.32)}$ are maintained; however, the interaction with Ser$^{190(4.57)}$ is lost. Such a binding orientation is not consistent with the data presented in Table 1.

(*S*)-D140 [(*S*)-12]. The reduction in binding affinity for the S190A mutation, 275-fold compared to WT, suggests a significant interaction between Ser$^{190(4.57)}$ and compound (*S*)-**12**. One feasible way (*S*)-**12** could interact with Ser$^{190(4.57)}$ and maintain interactions with Asp$^{138(3.32)}$ is shown in Figure 5. Although this binding orientation is similar to the one depicted for (*S*)-**10** in Figure 4, the aryloxy ring of (*S*)-**12** cannot directly interact with Tyr$^{356(7.43)}$ while (*S*)-**12** maintains interactions with Ser$^{190(4.57)}$ and Asp$^{138(3.32)}$ [the distance between the two phenyl rings of (*S*)-**12** is too short to accomplish this]. In addition, if (*S*)-**12** is moved to the left of the position shown in Figure 5 to form aromatic interactions with Tyr$^{356(7.43)}$, then not only is the hydrogen bond interaction with Ser$^{190(4.57)}$ lost but it is also quite difficult to position the long para-substituent of (*S*)-**12** into a pocket located between tms 1 and 2 (defined by residues Leu$^{65(1.39)}$, Ala$^{66(1.40)}$, Val$^{69(1.43)}$, Val$^{111(2.57)}$, Val$^{112(2.58)}$, Pro$^{113(2.59)}$, and Ala$^{116(2.62)}$). Thus, a direct aromatic interaction between (*S*)-**12** and Tyr$^{356(7.43)}$ appears to be unlikely. This is consistent with the relatively small reduction (15-fold, Table 1) in the (*S*)-**12** binding affinity for Y356A mutant receptors compared to the larger reduction in affinity experienced by compound **10** (10 000-fold). When docked into the rat β_1-AR as depicted in Figure 5, the amine substituent dimethoxyphenyl ring of (*S*)-**12** sits in a pocket defined by Thr$^{135(3.29)}$, Ser$^{136(3.30)}$, Val$^{137(3.31)}$, Asp$^{138(3.32)}$, Val$^{139(3.33)}$, Leu$^{140(3.34)}$, Ser$^{190(4.57)}$, Pro$^{193(4.60)}$, and Ile$^{194(4.61)}$. The *m*-methoxy oxygen is ideally situated to hydrogen bond to Ser$^{190(4.57)}$ and the *p*-methoxy oxygen to Ser$^{136(3.30)}$. Asp$^{138(3.32)}$ interacts with the amine nitrogen of (*S*)-**12**, and Asn$^{352(7.39)}$ can hydrogen bond with both the β-hydroxyl and aryloxy oxygen. The (*S*)-**12** aryloxy ring is located within the hydrophobic binding pocket defined by residues in tms 1, 2, 3, and 7 (Leu$^{65(1.39)}$, Met$^{107(2.53)}$, Val$^{111(2.57)}$, Val$^{112(2.58)}$, Gly$^{115(2.61)}$, Trp$^{134(3.28)}$, Asn$^{352(7.39)}$, Trp$^{353(7.40)}$, and Tyr$^{356(7.43)}$) and is able to form edge-to-face $\pi-\pi$ interactions with Trp$^{353(7.40)}$ but not Trp$^{134(3.28)}$ or Tyr$^{356(7.43)}$. The ether oxygen of the aryloxy para-substituent is able to interact with the backbone carbonyl group of both Val$^{112(2.58)}$ and Gly$^{115(2.61)}$. When binding in this orientation, (*S*)-**12**, like (*S*)-**10**, is situated higher in the receptor channel than the agonist catechol binding region.

Figure 5 depicts (*S*)-**12** maintaining an interaction with Asn$^{352(7.39)}$. For other para-substituted phenoxypropanolamines, such as compounds **4** and **5**, an interaction with Asn$^{352(7.39)}$ appears to be unlikely, since mutation of the equivalent residue in the β_2-AR, 5-HT$_{1A}$R, and 5-HT$_{1B}$R has no effect on binding affinity.[19,21,22] If an interaction with Asn$^{352(7.39)}$ is not necessary for (*S*)-**12** binding, the aryloxypropanol portion of the antagonist could easily adopt a different conformation from the one illustrated in Figure 5, resulting in the aryloxy moiety being located elsewhere in the ligand binding site (the antagonist is

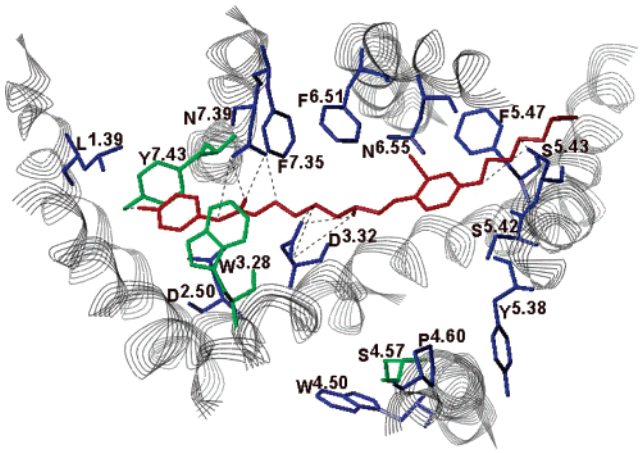

Figure 6. (*S*)-**9** (red) interactions with the WT rat β_1-AR model. In this binding mode Asn$^{352(7.39)}$ interacts with the urea functional group and the amine substituent phenyl ring sits in a hydrophobic pocket defined by Leu$^{65(1.39)}$, Met$^{107(2.53)}$, Val$^{111(2.57)}$, Val$^{112(2.58)}$, Gly$^{115(2.61)}$, Trp$^{134(3.28)}$, Asn$^{352(7.39)}$, Trp$^{353(7.40)}$, and Tyr$^{356(7.43)}$. The *p*-hydroxyl group of the amine substituent is able to interact with the hydroxyl group of Tyr$^{356(7.43)}$, and the amine substituent phenyl ring interacts with Trp$^{353(7.40)}$ and Tyr$^{356(7.43)}$ via edge-to-face $\pi-\pi$ interactions. Asp$^{138(3.32)}$ interacts with the β-hydroxyl and amine nitrogen of (*S*)-**9**. The (*S*)-**9** aryloxy para-substituent is located in a pocket between tms 5 and 6, enabling Ser$^{229(5.43)}$ to interact with both ether oxygens, and Ala$^{337(6.59)}$, Val$^{334(6.56)}$, Phe$^{338(6.60)}$, Ala$^{225(5.39)}$, and Ile$^{226(5.40)}$ surround the cyclopropyl group. The aryloxy ring interacts with Phe$^{329(6.51)}$ and Phe$^{330(6.52)}$ via edge-to-face $\pi-\pi$ interactions. The *o*-cyano group is pointing toward tm 6 and is located between Phe$^{329(6.51)}$ and Phe$^{330(6.52)}$. The color scheme and representations are the same as for Figure 2.

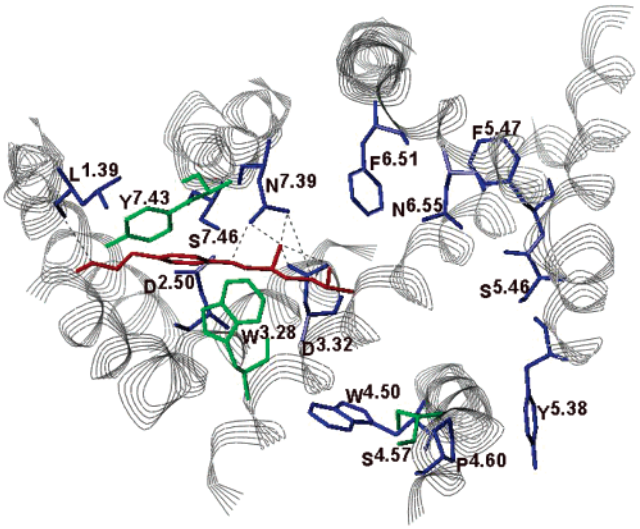

Figure 7. One possible orientation for (*S*)-**14** (red) in the WT rat β_1-AR model. Asp$^{138(3.32)}$ interacts with both the β-hydroxyl and amine nitrogen, whereas Asn$^{352(7.39)}$ can interact with the phenoxy oxygen, the β-hydroxyl, and the amine nitrogen of (*S*)-**14**. The phenoxy moiety is located in the tms 1, 2, 3, and 7 hydrophobic pocket (defined by Leu$^{65(1.39)}$, Met$^{107(2.53)}$, Val$^{111(2.57)}$, Val$^{112(2.58)}$, Gly$^{115(2.61)}$, Trp$^{134(3.28)}$, Asn$^{352(7.39)}$, Trp$^{353(7.40)}$, and Tyr$^{356(7.43)}$) and forms edge-to-face $\pi-\pi$ interactions with both Trp$^{353(7.40)}$ and Tyr$^{356(7.43)}$. The (*S*)-**14** para-substituent ether oxygen can hydrogen bond to the backbone carbonyl of Leu$^{65(1.39)}$, Val$^{112(2.58)}$, and Gly$^{115(2.61)}$. The isopropyl group is surrounded by Trp$^{134(3.28)}$, Thr$^{135(3.29)}$, Asp$^{138(3.32)}$, Trp$^{326(6.48)}$, Phe$^{329(6.51)}$, and Phe$^{348(7.35)}$. The color scheme and representations are the same as for Figure 2.

still able to maintain interactions with Asp$^{138(3.32)}$ and Ser$^{190(4.57)}$). In contrast, a tm 5 location of the (*S*)-**12** aryloxy moiety, similar to that reported for compound **13** in the β_2-AR,[33] is unlikely, since the interaction with Ser$^{190(4.57)}$ is lost when the (*S*)-**12** aryloxy moiety interacts with Tyr$^{224(5.38)}$. Such a binding orientation for (*S*)-**12** is not consistent with the binding affinity data (Table 1).

***(S)*-LK204-545 [(*S*)-9].** The binding affinity of compound **9** for the Y356A and Y356F mutant receptors (Table 1) indicates that, like compounds **7** and **10**, a direct aromatic interaction exists between this antagonist and Tyr$^{356(7.43)}$ and that the interaction is essential for maintaining an optimum binding mode (10 471-fold reduction in binding affinity for the Y356A mutant, compared to WT, and the restoration of the affinity by the Y356F mutant). (*S*)-**9** can be accommodated in the β_1-AR ligand binding site in a variety of orientations while maintaining interactions with Tyr$^{356(7.43)}$ and Asp$^{138(3.32)}$. In all orientations examined to date, (*S*)-**9** formed interactions with Asn$^{352(7.39)}$, whereas no interactions were observed with either Trp$^{134(3.28)}$ or Ser$^{190(4.57)}$. When docking (*S*)-**9** into the ligand binding site with the aryloxy moiety interacting with Tyr$^{356(7.43)}$, it was difficult to position the long para-substituent of (*S*)-**9** into the pocket located between tms 1 and 2 (defined by residues Leu$^{65(1.39)}$, Ala$^{66(1.40)}$, Val$^{69(1.43)}$, Val$^{111(2.57)}$, Val$^{112(2.58)}$, Pro$^{113(2.59)}$, and Ala$^{116(2.62)}$). However, the long para-substituent of (*S*)-**9** can be easily accommodated in the pocket located between tms 4 and 5 (defined by residues Leu$^{192(4.59)}$, Pro$^{193(4.60)}$, Ile$^{194(4.61)}$, Leu$^{195(4.62)}$, Asn$^{221(5.35)}$, and Tyr$^{224(5.38)}$) when the antagonist aryloxy moiety interacts with Tyr$^{224(5.38)}$, consistent with the orientation proposed by Wu et al. for compound **13** binding in the β_2-AR.[33] Yet another plausible binding orientation is depicted in Figure 6. In this orientation, the aryloxy para-substituent is located in a pocket between tms 5 and 6. When binding in this manner, interactions with Asp$^{138(3.32)}$ and Asn$^{352(7.39)}$ are formed and the amine substituent *p*-hydroxyphenyl ring of (*S*)-**9** is able to directly interact with Tyr$^{356(7.43)}$ via $\pi-\pi$ interactions and a hydrogen bond. The amino acid residues defining the binding pocket for the aryloxy para-substituent are listed in the caption for Figure 6; (*S*)-**9** adopts an extended conformation with the urea moiety interacting with Asn$^{352(7.39)}$, while both the amine nitrogen and the β-hydroxyl group can interact with Asp$^{138(3.32)}$. When binding in the extended conformation depicted in Figure 6, (*S*)-**9** occupies the full width of the receptor channel.

***(S)*-Metoprolol [(*S*)-14].** The way (*S*)-metoprolol [(*S*)-**14**] binds to the rat β_1-AR is not clear at this time. The data in Table 1 indicates that compound **14** makes no significant interactions with any of the three residues investigated in this study. Like (*S*)-**9**, (*S*)-**14** can be accommodated in the β_1-AR ligand binding site in a variety of orientations while maintaining interactions with Asp$^{138(3.32)}$. When (*S*)-**14** is docked into the WT rat β_1-AR with the para-substituted phenoxy ring located in the hydrophobic pocket near tms 1, 2, 3, and 7 (Figure 7), the para-substituent ether oxygen can hydrogen bond via the backbone carbonyl group of Leu$^{65(1.39)}$, Val$^{112(2.58)}$, and Gly$^{115(2.61)}$. The phenoxy ring interacts with both Trp$^{353(7.40)}$ and Tyr$^{356(7.43)}$ via edge-to-face $\pi-\pi$ interactions. As for the other compounds, Trp$^{134(3.28)}$ is not located in a position that allows a direct interaction with the (*S*)-**14** phenoxy ring, and Ser$^{190(4.57)}$ is physically too far away to interact with the antagonist in this orientation. The data in Table 1 suggests that if (*S*)-**14** adopts an orientation similar to that depicted in Figure 7, then the interaction with Tyr$^{356(7.43)}$ is not important for this antagonist. The absence of alternate interaction sites for the phenoxy ring make this orientation of (*S*)-**14** possible but unlikely. One plausible binding orientation for (*S*)-**14** is analogous to that depicted for the aryloxypropranolamine portion of (*S*)-**9** in Figure 6. In this orientation, the amine nitrogen is able to interact

with both Asp$^{138(3.32)}$ and Asn$^{352(7.39)}$, the β-hydroxyl interacts with Asp$^{138(3.32)}$, and the phenoxy oxygen can hydrogen bond to Asn$^{333(6.55)}$. Both Phe$^{329(6.51)}$ and Phe$^{330(6.52)}$ form edge-to-face $\pi-\pi$ aromatic interactions with the (*S*)-**14** phenoxy ring, and the para-substituent is located in a pocket near tms 5 and 6 defined by Ala$^{225(5.39)}$, Ser$^{229(5.43)}$, Asn$^{333(6.55)}$, Val$^{334(6.56)}$, and Ala$^{337(6.59)}$. The para-substituent ether oxygen is able to interact with Ser$^{229(5.43)}$ and the backbone carbonyl of Ala$^{225(5.39)}$. Like (*S*)-**9**, yet another possible binding orientation for (*S*)-**14** involves an edge-to-face $\pi-\pi$ aromatic interaction with Tyr$^{224(5.38)}$. When binding in this manner, the amine nitrogen and β-hydroxyl both interact with Asp$^{138(3.32)}$, and the para-substituent is located in a pocket near tms 4 and 5 (defined by Leu$^{192(4.59)}$, Pro$^{193(4.60)}$, Leu$^{195(4.62)}$, Asn$^{221(5.34)}$, and Tyr$^{224(5.38)}$). Such an (*S*)-**14** orientation is consistent with the proposed binding orientation of compound **13** in the β_2-AR.[33]

Discussion

The ligand binding pocket of the β-ARs is thought to be formed by the juxtaposition of the seven tm regions.[36] The smaller shifts in antagonist binding affinities for the mutant receptors (decreases of $\leq$15-fold compared to WT, Table 1) could indicate the loss of weak interactions between the mutated residues and the antagonist, or alternatively, they may reflect the effect of the mutations on the overall alignment and stabilization of the receptor conformation.[14]

The large binding affinity decreases observed for the mutant receptors are more likely to be due to the loss of significant interactions between the mutated residues and the antagonist. Mutation of Tyr$^{356(7.43)}$ to Ala produced 55−10 471-fold reductions in the binding affinity for compounds **1**, **7**, **9**, **10**, and **11** compared to the WT receptor (Table 1), suggesting that significant interaction points between the receptor and the antagonists have been removed.[22,37−39] The binding affinities of these antagonists were restored almost to WT levels in the Y356F mutant, indicating that the interaction with Tyr$^{356(7.43)}$ is predominately aromatic (Table 1). The dramatic reductions in binding affinities observed for compounds **7**, **9**, and **10** for the Y356A mutant receptor (6310−10 471-fold compared to the WT receptor) may also reflect the importance of Tyr$^{356(7.43)}$ in maintaining the antagonist in an optimum binding orientation and/or the inability of an antagonist to adopt an effective alternative binding orientation once Tyr$^{356(7.43)}$ is removed. It seems likely that the aromatic interaction with Tyr$^{356(7.43)}$ (or Phe$^{356(7.43)}$) orientates the antagonist to maximize the interactions it makes with Asp$^{138(3.32)}$, Asn$^{352(7.39)}$, and other binding site residues.

The competitive antagonists **1**, **7**, and **11** contain only one aryl moiety, and if they are to form aromatic interactions with Tyr$^{356(7.43)}$, they must be orientated with the aryloxy moiety located in the tms 1, 2, 3, and 7 hydrophobic pocket [a binding orientation analogous to that depicted for (*S*)-**8** in Figure 2]. Such a binding orientation is also consistent with the previous site-directed mutagenesis and structure−activity studies carried out for Asn$^{(7.39)}$.[16−20,22] When an antagonist interacts with Asp$^{138(3.32)}$ and is located with the aryloxy moiety in the tms 1, 2, 3, and 7 hydrophobic pocket, then Asn$^{352(7.39)}$ is ideally positioned to interact with the aryloxy oxygen and/or the β-hydroxyl group.

The two other competitive antagonists in this study to demonstrate significant interactions with Tyr$^{356(7.43)}$ are compounds **9** and **10**. Both of these compounds contain two aryl moieties and thus have two alternative ways to aromatically interact with Tyr$^{356(7.43)}$. For (*S*)-**10** there is an additional significant interaction with Ser$^{190(4.57)}$, which helps to orientate the antagonist within the rat β_1-AR. The (*S*)-**10** orientation depicted in Figure 4 is consistent with the data presented in Table 1. In contrast, the situation with compound **9** is unclear. (*S*)-**9** can be accommodated within the β_1-AR ligand binding site with either aryl moiety interacting with Tyr$^{356(7.43)}$. One possible binding orientation for (*S*)-**9** is illustrated in Figure 6.

Our data support the observations, but only partially support the conclusions, of an earlier report[11] that Ser$^{190(4.57)}$ is not required for competitive antagonist binding in the rat β_1-AR. The earlier report was based solely on saturation studies of compound **8** in the human β_2-AR. We confirmed that there was no difference in the binding affinity of compound **8** between the S190A mutant and the WT rat β_1-AR (Table 1). Regardless of the binding orientation adopted, it is physically impossible for (*S*)-**8** to interact with Ser$^{190(4.57)}$ while maintaining interactions with Asp$^{138(3.32)}$ (for example refer to Figure 2). Similarly, the binding affinities and docking studies for compounds **1**, **7**, **9**, **11**, and **14** indicate that Ser$^{190(4.57)}$ is unlikely to be an interaction point for these antagonists (Table 1 and Figures 6 and 7). In contrast, however, Ser$^{190(4.57)}$ was an important interaction site for two antagonists in this study. The binding affinities of (*S*)-**12** and compound **10** were reduced by 275- and 690-fold, respectively, for the S190A mutant (Table 1), suggesting that these two antagonists interact directly with Ser$^{190(4.57)}$. The modeling studies confirmed that, while the antagonists maintained interactions with Asp$^{138(3.32)}$, the *m*-methoxy group of (*S*)-**12** and the *m*-amide group of (*S*)-**10** are able to hydrogen bond with the side chain of Ser$^{190(4.57)}$ (Figures 5 and 4, respectively).

Although the binding affinity data indicate that (*S*)-**12** makes a significant interaction with Ser$^{190(4.57)}$, there do not appear to be any interactions with the two other residues mutated in this study. When the phenoxy moiety of (*S*)-**12** is located near tms 3 and 4, an interaction with Ser$^{190(4.57)}$ is not possible while maintaining interactions with Asp$^{138(3.32)}$. However, interactions with both Asp$^{138(3.32)}$ and Ser$^{190(4.57)}$ can be formed when the dimethoxyphenyl moiety of the (*S*)-**12** amine substituent is located near tms 3 and 4, as in Figure 5. When adopting the orientation depicted in Figure 5, the para-substituted phenoxy ring cannot reach Tyr$^{356(7.43)}$, and the exact location of the phenoxy moiety is unclear at this time. In Figure 5 we have orientated the compound so that the phenoxy para-substituent is located in the tms 1, 2, 3, and 7 hydrophobic pocket; however, this is only one possibility.

In contrast to (*S*)-**12**, compound **14** does not appear to interact significantly with any of the three residues mutated in this study (Table 1). (*S*)-**14** can be orientated with the phenoxy moiety in the tms 1, 2, 3, and 7 hydrophobic pocket (as in Figure 7); however, we would expect Tyr$^{356(7.43)}$ to play a more important role in antagonist binding if this orientation was adopted. Alternatively, (*S*)-**14** could adopt an orientation similar to that of the aryloxypropanolamine portion of (*S*)-**9** in Figure 6. Another possible binding orientation is one where the para-substituted phenoxy ring is located near tms 4 and 5, with the phenyl ring interacting with Tyr$^{224(5.38)}$. Such an orientation is analogous to the proposed binding mode of compound **13** in the β_2-AR.[33]

Like compound **14**, compound **8** does not interact significantly with any of the three residues examined in this study and the data does not clearly distinguish between a number of possible binding orientations (Table 1). Compound **8** may adopt a binding orientation similar to that of the structural analogue **7**; where the aryloxy moiety is located in the tms 1, 2, 3 and 7

hydrophobic pocket as illustrated in Figure 2. When binding in this orientation the iodine atom is located in a pocket defined by $Met^{107(2.53)}$, $Val^{111(2.57)}$, $Asp^{138(3.32)}$, $Cys^{141(3.35)}$, $Trp^{326(6.48)}$, $Gly^{355(7.42)}$, and $Ser^{359(7.46)}$ (Figures 2 and 3) and may serve to anchor the antagonist in the receptor via steric and/or noncovalent interactions. The iodine atom of compound **8** does not appear to interact directly with $Tyr^{356(7.43)}$ and the small effect of mutating this residue on the pK_d of compound **8** suggests at least two possibilities: (1) the iodine atom weakens the strength of the aromatic interaction with $Tyr^{356(7.43)}$ or (2) compound **8** adopts an alternative orientation in the receptor, as was our original hypothesis.[25]

Overall, the data indicate clearly that a number of competitive antagonists bind with their aryloxy moieties located in a hydrophobic pocket defined by residues in tms 1, 2, 3, and 7. Such a binding orientation also enables interaction with $Asn^{352(7.39)}$, consistent with previous site-directed mutagenesis and structure−activity studies.[16−20,22] In contrast, recent β_2-AR photoaffinity labeling studies with compound **13** have indicated that the aryloxy moiety of this antagonist is located near tms 4 and 5 and interacts with $Tyr^{(5.38)}$.[33] Together these data support the conclusion that competitive antagonists can bind in at least two orientations to the β_1-AR. We have not yet identified the precise location of the aryloxy moieties of compounds **8**, **9**, and **14** within the ligand binding site. The binding affinity data and the modeling presented here have identified residues for future site-directed mutagenesis studies that may help to further delineate the binding orientations of antagonists, for example $Ser^{359(7.46)}$ (possible interactions with compounds **7**−**9**), $Met^{107(2.53)}$ (compounds **7** and **8**), $Tyr^{224(5.38)}$ (compounds **8**, **9**, and **14**), and $Phe^{329(6.51)}$ (compounds **8**, **9**, and **14**).

Conclusion

The results presented here demonstrate that $Tyr^{356(7.43)}$ and $Ser^{190(4.57)}$ play distinct and important roles in binding competitive β_1-AR antagonists. $Ser^{190(4.57)}$ was a significant interaction site for two of the antagonists studied, i.e., compounds **10** and (*S*)-**12**. $Tyr^{356(7.43)}$, which is part of a hydrophobic pocket involving tms 1, 2, 3, and 7, appears to be a significant aromatic interaction site for compounds **1**, **7**, **9**, **10**, and **11**, whereas interaction with $Tyr^{356(7.43)}$ is not important for **8**, (*S*)-**12**, and **14** binding. Although it is also part of the tm 1, 2, 3, and 7 hydrophobic pocket, $Trp^{134(3.28)}$ does not appear to play a significant role in competitive antagonist binding. The results therefore extend our understanding of how competitive β_1-AR antagonists bind to the tms 1, 2, 3, and 7 hydrophobic pocket; highlight the importance of $Tyr^{356(7.43)}$ as an interaction site; and demonstrate the involvement of tm 4 in competitive antagonist binding.

Experimental Section

Materials. Glutamine, HEPES, and compounds **1** and **10** were purchased from Sigma Chemical Co. Compounds **7** and **11** were obtained from Tocris Cooksen Ltd. Compounds **9**, **12**, and **14** were synthesized in our laboratory by Dr. Dimitri Iakovidis according to the published procedures.[30,31,40] All synthesized compounds were checked by TLC, HPLC, NMR, elemental analysis, and mass spectroscopy, and their physical characteristics were consistent with their chemical structure.[30,31,40] Unless otherwise indicated, the racemates were used. Compound **8** was produced using the chloramine-T/NaI method.[41] Oligonucleotides, geneticin (G418), and the mammalian expression vector pcDNA3.1 were obtained from Invitrogen. Chinese hamster ovary (CHO) cell line, fetal calf serum, and bovine serum albumin (BSA) (fraction V) were obtained from the Commonwealth Serum Laboratories (CSL). Hams F12, sodium pyruvate, trypsin, penicillin, and streptomycin were obtained from Edward Keller. Restriction enzymes *EcoR* 1 and *Xba* 1 were purchased from Promega Corp. The plasmid construct pGem3Z-β_1 encoding for the rat β_1-AR was provided by Dr. Curtis A. Machida. Quik change site-directed mutagenesis kit was purchased from Stratagene. All other chemicals were of reagent grade from BDH Chemicals.

Site-Directed Mutagenesis. For β_1-AR expression in CHO cells, the entire coding region derived from pGem3Z-β_1 (base pairs −82 to +1573) was inserted into the *EcoR* 1 and *Xba* 1 sites of the mammalian vector pcDNA3.1, which provides G418 selection. Site-directed mutagenesis for amino acids $Trp^{134(3.28)}$, $Ser^{190(4.57)}$, and $Tyr^{356(7.43)}$ to W134A, S190A, Y356A, and Y356F was performed using the Quik change method according to the manufacturer's instructions. The identities of the mutations were confirmed by automated sequencing on an ABI sequencer.

Cell Culture and Transfection. Permanent lines of stably expressing cells were maintained in a monolayer culture in Hams F12 media supplemented with 10% fetal calf serum, 2 mM glutamine, 1 mM sodium pyruvate, 100 units/mL penicillin, 100 μg/mL streptomycin, and 800 μg/mL G418 in a 10% CO_2 incubator at 37 °C. WT and mutant receptor plasmids were stably transfected into CHO cells by electroporation. Transfected clones were selected in the presence of 800 μg/mL G418. Colonies originating from single cells were subcloned and evaluated for receptor expression using ^{125}I-CYP (compound **8**) binding.

Preparation of Crude Cell Membranes. Membranes were prepared from preconfluent, stably transfected CHO cells. The cells were washed twice with ice-cold phosphate buffer solution and harvested with 25 mM Tris-HCl, pH 7.5, 1 mM EDTA buffer, homogenized with 20 strokes of a Dounce pestle and then centrifuged at 10 000*g* for 15 min. The final membrane pellets were resuspended in Hank's balanced salt solution and stored at −80 °C until needed.[42] Cells were thawed as required and resuspended in Hank's balanced salt solution supplemented with 20 mM HEPES and 0.1% (mass/vol) BSA at 100−200 μg protein/mL. Protein content was determined by the Bradford method[43] using BSA as the standard.

Radioligand Binding Studies. In saturation-binding studies, 0.1 mL of membranes was incubated in duplicate with nine different concentrations of ^{125}I-CYP (compound **8**, 2 pM−1 nM). Competition binding experiments were conducted as previously described.[42] Cell membranes were incubated with 100 pM compound **8** and various concentrations of displacing ligand, in a final volume of 0.2 mL. All determinations in the binding assays were done in triplicate. Membranes were incubated for 1 h at 37 °C in the dark and the assay terminated by rapid filtration over glass fiber filters presoaked with (0.1%) polyethyleneimine. Nonspecific binding was determined in the presence of 10 μM compound **1**.

Data Analysis. Data are expressed as the mean ± standard error of the mean (SEM) of three to five independent experiments. Dissociation constant (K_d) (saturation studies), inhibition constant (K_i) (drug inhibition), and receptor binding density (B_{max}) values were determined using the computerized iterative curve-fitting program EBDA version 4.0, which incorporates LIGAND version 4.0.[44,45] Pseudo-Hill coefficients (n_H) were obtained from analysis of binding data using the sigmoidal fit function of the EBDA program.

Statistical Analysis. The pK_d, pK_i, and B_{max} values in the mutant versus WT receptors were compared by one-way ANOVA followed by pairwise Tukey's test using the Analyse-it software for Microsoft Excel.[46] Critical values of $p < 0.05$ defined statistical significance.

Homology Modeling of the WT Rat β_1-AR. Model construction and antagonist docking were carried out on a Silicon Graphics O^2 Unix workstation. The construction and validation of the WT rat β_1-AR model have been described in detail elsewhere,[14] so only a brief outline will be given here. The seven tm sequences of the rat and human β_1-AR, human β_2-AR, and bovine rhodopsin were aligned[14] in a manner consistent with Palczewski et al.[32] The amino acid sequence of the A chain of the bovine rhodopsin crystal structure (PDB file 1F88, resolution 2.8 Å) was mutated to that of

the rat β_1-AR using the mutate functionality in the Biopolymer module of the modeling program SYBYL (version 6.8/6.9).[47] The crude rat β_1-AR model was then subjected to molecular mechanics minimization using the following parameters: Kollman all atom force field and atomic charges, conjugate gradient minimization, distance dielectric function, 8-Å nonbonded cutoff, and 2000 maximum iterations. After minimization the rat β_1-AR model was superimposed onto the 1F88 bovine rhodopsin crystal structure via the A chain backbone atoms and the resulting root mean square was 0.8 Å.[48]

To construct the model of the Y356A mutant rat β_1-AR, $Tyr^{356(7.43)}$ in the crude WT model was mutated to Ala and the resulting crude Y356A model was minimized using the same protocol as that described above for the WT rat β_1-AR model. The size and shape of the ligand binding pockets in both the WT and Y356A rat β_1-AR models were examined using Connolly surfaces generated within SYBYL using the default parameters.

Docking Competitive Antagonists into the β_1-AR Model. The competitive antagonists were constructed within the sketch functionality of SYBYL in a fully extended conformation. The (*S*)-isomers of the aryloxypropanolamines were used as they are known to have the highest affinity for the β_1-AR. All structures were fully optimized using the following protocol: (1) the Tripos molecular mechanics force field and Gasteiger−Huckel atomic charges within SYBYL (all other parameters were left at the default values) were used; (2) the AM1 Hamiltonian within the MOPAC (version 6.00)[49] program as supplied with SYBYL (the parameters used for the MOPAC semiempirical molecular orbital calculations were AM1 Hamiltonian, precise convergence, no molecular mechanics correction for amide linkages, and full geometry optimization) was utilized; (3) calculations were done at the B3LYP level[50] with the 6-31G* basis set for C, N, O, S, F, and H atoms and 3-21G* for I atoms (hereafter referred to as 6-31G* for simplicity) within the Gaussian 98[51] or 03 program packages;[52] and finally (4) the resulting B3LYP geometries were then subjected to single point calculations at the MP2 level[53] (MP2/6-31G*//B3LYP/6-31G*).

The individual antagonists were then manually docked into the WT rat β_1-AR model with the assumption that interactions with $Asp^{138(3.32)}$ were essential for competitive antagonist binding.[6] Wherever possible, antagonist interactions with $Asn^{352(7.39)}$ were maintained throughout the docking process. The antagonist torsion angles were allowed to vary in order to maximize the putative antagonist/receptor interactions. For hydrogen-bond interactions, donor−acceptor distances of 3.0−4.0 Å were considered to be feasible. Distances of 4.0−7.0 Å between ring centroids were deemed acceptable for aromatic−aromatic interactions.

Once the antagonist was docked into the β_1-AR model, the entire antagonist/receptor complex was subjected to molecular mechanics minimization, following the same protocol as for the model construction, with the exceptions that the MMFF94 force field, MMFF94 atomic charges, and 1000 maximum iterations were used. For each antagonist different binding modes were examined.

The antagonist molecules were extracted out of the minimized antagonist/receptor complex, and the energy was calculated for the bound antagonist conformation after partial geometry optimization (all torsion angles were kept fixed, and only the bond lengths and bond angles were optimized) at the B3LYP theory level, followed by single point calculations at the MP2 theory level as described above for the extended antagonist conformations. For each antagonist, the energy of the various bound conformations were compared to the energy of the fully extended conformation to ensure that the bound conformation was energetically feasible (i.e., within 15 kcal/mol of the fully extended conformation; bound conformations higher in energy than this were considered to be unrealistic and were discarded). The energy differences between the extended and bound antagonist conformations are reported in the Supporting Information.

Acknowledgment. We thank Mr. David Casley for iodinating cyanopindolol and Ms. Heddy Wilshire for excellent technical assistance. This work was supported through grants from the Austin Hospital Medical Research Foundation, the Sir Edward Dunlop Foundation, and the Australian Partnership for Advanced Computing National Facility (APAC). S.N.S.L. was supported by a National Health and Medical Research Council of Australia, INSERM Fellowship.

Supporting Information Available: Table listing the energy differences between the fully extended and bound antagonist conformations. This material is available free of charge via the Internet at http://pubs.acs.org.

References

(1) Gether, U. Uncovering molecular mechanisms involved in activation of G protein coupled receptors. *Endocr. Rev.* **2000**, *21*, 90−113.

(2) Hannawacker, A.; Krasel, C.; Lohse, M. J. Mutation of Asn293 to Asp in transmembrane helix VI abolishes agonist-induced but not constitutive activity of the β_2-adrenergic receptor. *Mol. Pharmacol.* **2002**, *62*, 1431−1437.

(3) Karnik, S. S.; Gogonea, C.; Patil, S.; Saad, Y.; Takezako, T. Activation of G-protein-coupled receptors: A common molecular mechanism. *Trends Endocr. Metab.* **2003**, *14*, 431−437.

(4) Chen, S.; Lin, F.; Xu, M.; Riek, P.; Novotny, J.; Graham, R. M. Mutation of a single TMV1 residue, Phe^{282}, in the β_2-adrenergic receptor results in structurally distinct activated receptor conformations. *Biochemistry* **2002**, *41*, 6045−6053.

(5) Swaminath, G.; Xiang, Y.; Lee, T. W.; Steenhuis, J.; Parnot, C.; Kobilka, B. K. Sequential binding of agonists to the β_2-adrenoceptor. Kinetic evidence for intermediate conformational states. *J. Biol. Chem.* **2004**, *279*, 686−691.

(6) Dixon, R. A. F.; Sigal, I. S.; Strader, C. D. Structure−function analysis of the β-adrenergic receptor. *Cold Spring Harbor Symp. Quant. Biol.* **1988**, *3*, 487−497.

(7) Sugimoto, Y.; Fujisawa, R.; Tanimura, R.; Lattion, A. L.; Cotecchia, S.; Tsujimoto, G.; Nagao, T.; Kurose, H. β_1-selective agonist (−)-1-(3,4-dimethoxyphenethylamino)-3-(3,4-dihydroxy)-2-propanol [(−)-RO363] differentially interacts with key amino acids responsible for β_1-selective binding in resting and active states. *J. Pharmacol. Exp. Ther.* **2002**, *301*, 51−58.

(8) Strader, C. D.; Candalore, M. R.; Hill, W. S.; Dixon, R. A. F.; Sigal, I. S. Identification of two serine residues involved in agonist activation of the β-adrenergic receptor. *J. Biol. Chem.* **1989**, *264*, 13572−13578.

(9) Liapakis, G.; Ballesteros, J. A.; Papachristou, S.; Chan, W. C.; Chen, X.; Javitch, J. A. The forgotten serine: A critical role for Ser^{203} in ligand binding to and activation of the β_2-adrenergic receptor. *J. Biol. Chem.* **2000**, *275*, 37779−37788.

(10) Del Carmine, R.; Ambrosio, C.; Sbraccia, M.; Cotecchia, S.; Ijzerman, A. P.; Costa, T. Mutations inducing divergent shifts of constitutive activity reveal different modes of binding among catecholamine analogues to the β_2-adrenergic receptor. *Br. J. Pharmacol.* **2002**, *135*, 1715−1722.

(11) Wieland, K.; Zuurmond, H. M.; Krasel, C.; Ijzerman, A. P.; Lohse, M. J. Involvement of Asn-293 in stereospecific agonist recognition and in activation of the beta 2-adrenergic receptor. *Proc. Natl. Acad. Sci. U.S.A.* **1996**, *93*, 9276−9281.

(12) Lewell, X. Q. A model of the adrenergic beta-2 receptor and binding sites for agonist and antagonist. *Drug Des. Discovery* **1992**, *9*, 29−48.

(13) Trumpp-Kallmeyer, S.; Hoflack, J.; Bruinvels, A.; Hibert, M. Modeling of G-protein-coupled receptors: Application to dopamine, adrenaline, serotonin, acetylcholine, and mammalian opsin receptors. *J. Med. Chem.* **1992**, *35*, 3448−3462.

(14) Rezmann-Vitti, L. A.; Louis, S. N. S.; Nero, T. L.; Jackman, G. P.; Iakovidis, D.; Machida, C. A.; Louis, W. J. Agonist binding and activation of the rat β_1-adrenergic receptor: Role of $Trp^{134\ (3.28)}$, $Ser^{190\ (4.57)}$ and $Tyr^{356\ (7.43)}$. *Biochem. Pharmacol.* **2004**, *68*, 675−688.

(15) For the rat β_1-AR, the residues involved in agonist binding are $Asp^{138(3.32)}$, which interacts with the agonist amino group (refs 2, 5−7); $Ser^{228(5.42)}$, $Ser^{229(5.43)}$ and $Ser^{232(5.46)}$, which hydrogen bond with the hydroxyl groups of the agonist's catechol moiety (refs 2, 5-10); $Asn^{333(6.55)}$, which stereospecifically interacts with the agonist β-hydroxyl group (refs 2, 11); and $Phe^{233(5.47)}$, $Phe^{329(6.51)}$, and $Phe^{330(6.52)}$, which form an aromatic pocket into which the agonist's catechol ring can be accommodated (refs 6, 12, 13). For the rat β_1-AR, the amino acid residues have been dually numbered according to the nomenclature of Ballesteros and Weinstein (Ballesteros, J. A.; Weinstein, H. Integrated methods for the construction of three-dimensional models and computational probing of structure−function relations in G protein-coupled receptors. *Methods Neurosci.* **1995**, *25*, 366−428). In superscript they are numbered according to their position in the receptor sequence, and in parentheses they have been

given a number corresponding to their relative position in the helix. In this universal numbering system, every amino acid number begins with the tm number, followed by a number that defines their position relative to the most conserved residue in that tm. The reference residue is assigned the number 50. To avoid confusion, amino acid residues in other receptors are numbered only using the universal numbering system.

(16) Guan, X. M.; Peroutka, S. J.; Kobilka, B. K. Identification of a single amino acid residue responsible for the binding of a class of beta-adrenergic receptor antagonists to 5-hydroxytryptamine$_{1A}$ receptors. *Mol. Pharmacol.* **1992**, *41*, 695−698.

(17) Elling, C. E.; Thirstrup, K.; Holst, B.; Schwartz, T. W. Conversion of agonist site to metal-ion chelator site in the β_2-adrenergic receptor. *Proc. Natl. Acad. Sci. U.S.A.* **1999**, *96*, 12322−12327.

(18) Glennon, R. A.; Dukat, M.; Westkaemper, R. B.; Ismaiel, A. M.; Izzarelli, D. G.; Parker, E. M. The binding of propranolol at 5-hydroxytryptamine$_{1D\beta}$ T355N mutant receptors may involve formation of two hydrogen bonds to asparagine. *Mol. Pharmacol.* **1996**, *49*, 198−206.

(19) Suryanarayana, S.; Daunt, D. A.; Von Zastrow, M.; Kobilka, B. K. A point mutation in the seventh hydrophobic domain of the α_2 adrenergic receptor increases its affinity for a family of β receptor antagonists. *J. Biol. Chem.* **1991**, *266*, 15488−15492.

(20) Kuipers, W.; Link, R.; Standaar, P. J.; Stoit, A. R.; Van Wijngaarden, I.; Leurs, R.; Ijzerman, A. P. Study of the interaction between aryloxypropanolamines and Asn386 in helix VII of the human 5-hydroxytryptamine$_{1A}$ receptor. *Mol. Pharmacol.* **1997**, *51*, 889−896.

(21) Langlois, M.; Bremont, B.; Rousselle, D.; Gaudy, F. Structural analysis by the comparative molecular field analysis method of the affinity of β-adrenoceptor blocking agents for 5-HT$_{1A}$ and 5-HT$_{1B}$ receptors. *Eur. J. Pharmacol.* **1993**, *244* , 77−87.

(22) Suryanarayana, S.; Kobilka, B. K. Amino acid substitutions at position 312 in the seventh hydrophobic segment of the β_2-adrenergic receptor modify ligand-binding specificity. *Mol. Pharmacol.* **1993**, *44*, 111−114.

(23) Ijzerman, A. P.; Zuurmond, H. M. Molecular modelling of β-adrenoceptors. In *Membrane Protein Models: Experiment, Theory and Speculation*; Findlay, J. Ed.; BIOS Scientific Publishers: Oxford, 1996; pp 133−144.

(24) Kuipers, W.; Van Wijngaarden, I.; Ijzerman, A. P. A model of the serotonin 5-HT$_{1A}$ receptor: Agonist and antagonist binding sites. *Drug Des. Discovery* **1994**, *11*, 231−249.

(25) Rezmann-Vitti, L. A.; Louis, S. N. S.; Nero, T. L.; Jackman, G. P.; Machida, C. A.; Louis, W. J. Site-directed mutagenesis of the rat β_1-adrenoceptor. Involvement of Tyr$^{356(7.43)}$ in (±)cyanopindolol but not (±)[^{125}Iodo]cyanopindolol binding. *Eur. J. Med. Chem.* **2004**, *39*, 625−631.

(26) Lu, Z. L.; Saldanha, J. W.; Hulme, E. C. Transmembrane domains 4 and 7 of the M_1 muscarinic acetylcholine receptor are critical for ligand binding and the receptor activation switch. *J. Biol. Chem.* **2001**, *276*, 34098−34104.

(27) Javitch, J. A.; Shi, L.; Simpson, M. M.; Chen, J.; Chiappa, V.; Visiers, I.; Weinstein, H.; Ballesteros, J. A. The fourth transmembrane segment of the dopamine D_2 receptor: Accessibility in the binding-site crevice and position in the transmembrane bundle. *Biochem.* **2000**, *39*, 12190−12199.

(28) Horn, F.; Vriend, G.; Cohen, F. E. Collecting and harvesting biological data: The GPCRDB and NucleaRDB information systems. *Nucl. Acids Res.* **2001**, *29*, 346−349.

(29) Louis, S. N.; Rezmann-Vitti, L. A.; Nero, T. L.; Iakovidis, D.; Jackman, G. P.; Louis, W. J. Affinity and CoMFA analysis of a series of phenoxypropranolamines for the human β_1-adrenoceptors. *Eur. J. Med. Chem.* **2002**, *37*, 111−125.

(30) Jackman, G. P.; Iakovidis, D.; Nero, T. L.; Anavekar, N. S.; Rezmann-Vitti, L. A.; Louis, S. N. S.; Mori, M.; Drummer, O. H.; Louis, W. J. Synthesis, β-adrenoceptor pharmacology and toxicology of *S*-(−)-1-(4-(2-ethoxyethoxy)phenoxy)-2-hydroxy-3-(2-(3,4-dimethoxyphenyl)ethylamino)propane hydrochloride, a short acting β_1-specific antagonist. *Eur. J Med. Chem.* **2002**, *37*, 731−741.

(31) Berthold, R.; Louis, W. J. 3-Aminopropoxyphenyl derivatives and pharmaceutical compositions containing them. US Patent 4425362, 1984.

(32) Palczewski, K.; Kumasaka, T.; Hori, T.; Behnke, C. A.; Motoshima, H.; Fox, B. A.; Le Trong, I.; Teller, D. C.; Okada, T.; Stenkamp, R. E.; Yamamoto, M.; Miyano, M. Crystal structure of rhodopsin: A G protein-coupled receptor. *Science* **2000**, *289*, 739−745.

(33) Wu, Z.; Thiriot, D. S.; Ruoho, A. E. Tyr^{199} in transmembrane domain 5 of the β_2-adrenergic receptor interacts directly with the pharmacophore of a unique fluorenone-based antagonist. *Biochem. J.* **2001**, *354*, 485−491.

(34) Waugh, D. J.; Gaivin, R. J.; Zuscik, M. J.; Gonzalez-Cabrera, P.; Ross, S. A.; Yun, J.; Perez, D. M. Phe-308 and Phe-312 in transmembrane domain 7 are major sites of α_1-adrenergic receptor antagonist binding. *J. Biol. Chem.* **2001**, *276*, 25366−25371.

(35) Ishiguro, M.; Futabayashi, Y.; Ohnuki, T.; Ahmed, M.; Muramatsu, I.; Nagatomo, T. Identification of binding sites of prazosin, tamsulosin and KMD-3213 with α_1-adrenergic receptor subtypes by molecular modeling. *Life Sci.* **2002**, *71*, 2531−2541.

(36) Wong, S. K. F.; Claughter, C.; Ruoho, A. E.; Ross, E. M. The catecholamine binding site of the β-adrenergic receptors is formed by juxtaposed membrane spanning domains. *J. Biol. Chem.* **1988**, *263*, 7925−7928.

(37) Fersht, A. R. Relationships between apparent binding energies measured in site-directed mutagenesis experiments and energetics of binding and catalysis. *Biochemistry* **1988**, *27*, 1577−1580.

(38) Meyer, E. A.; Castellano, R. K.; Diederich, F. Interactions with Aromatic Rings in Chemical and Biological Recognition. *Angew. Chem., Int. Ed.* **2003**, *42*, 1210−1250.

(39) Serrano, L.; Bycroft, M.; Fersht, A. R. Aromatic−aromatic interactions and protein stability. Investigation by double-mutant cycles. *J. Mol. Biol.* **1991**, *218*, 465−475.

(40) Carlsson, P. A. E.; Brandstrom, A. E.; Lamm, B. R.; Ablad, B. A. H.; Carlsson, S. A. I.; Corrodi, H. R.; Ek, L. 1-(Alkylamino)-3-(*p*-alkoxyphenoxy)-2-propanols as β-blockers in heart diseases. German patent DE 2020864, 1970.

(41) Lew, R.; Summers, R. J. Autoradiographic localisation of β-adrenoceptor subtypes in guinea-pig kidney. *Br. J. Pharmacol.* **1985**, *85*, 341−348.

(42) Blin, N.; Camoin, L.; Maigret, B.; Strosberg, A. D. Structural and conformational features determining selective signal transduction in the β_3-adrenergic receptor. *Mol. Pharmacol.* **1993**, *44*, 1094−1104.

(43) Bradford, M. M. A rapid and sensitive method for the quantitation of microgram quantities of protein utilizing the principle of protein−dye binding. *Anal. Biochem.* **1976**, *72*, 248−254.

(44) McPherson, G. A. A practical computer-based approach to the analysis of radioligand binding experiments. *Comput. Programs Biomed.* **1983**, *17*, 107−113.

(45) Munson, P. J.; Rodbard, D. LIGAND: A versatile computerised approach for the characterisation of ligand binding systems. *Anal. Biochem.* **1980**, *109*, 220−239.

(46) Analyse-it, General statistics software for Microsoft Excel, Analyse-It Software Ltd., PO Box 103, Leeds LS27 7WZ, England.

(47) Sybyl 6.8/6.9/7.0, Tripos Inc., 1699 South Hanley Road, St. Louis, MO 63144, USA.

(48) Since the construction of the WT rat β_1-AR model,[14] two higher resolution bovine rhodopsin crystal structures have become available (1GZM, resolution 2.65 Å, and 1U19, resolution 2.2 Å). Superimposition of the model template, i.e., the A chain of 1F88, with either 1GZM or 1U19 via the backbone atoms indicates little variation between the backbone atoms of the three crystal structures (rms < 1.1 Å between 1F88 and either 1GZM or 1U19).

(49) Mopac 6.00, as supplied within Sybyl 6.8/6.9/7.0.

(50) (a) Lee, C.; Yang, W.; Parr, R. G. Development of the Colle-Salvetti correlation-energy formula into a functional of the electron density. *Phys. Rev. B* **1988**, *37*, 785−789. (b) Becke, A. D. Density-functional thermochemistry. III. The role of exact exchange. *J. Chem. Phys.* **1993**, *98*, 5648−5652.

(51) Frisch, M. J.; Trucks, G. W.; Schlegel, H. B.; Scuseria, G. E.; Robb, M. A.; Cheeseman, J. R.; Zakrzewski, V. G.; Montgomery, J. A., Jr.; Stratmann, R. E.; Burant, J. C.; Dapprich, S.; Millam, J. M.; Daniels, A. D.; Kudin, K. N.; Strain, M. C.; Farkas, O.; Tomasi, J.; Barone, V.; Cossi, M.; Cammi, R.; Mennucci, B.; Pomelli, C.; Adamo, C.; Clifford, S.; Ochterski, J.; Petersson, G. A.; Ayala, P. Y.; Cui, Q.; Morokuma, K.; Malick, D. K.; Rabuck, A. D.; Raghavachari, K.; Foresman, J. B.; Cioslowski, J.; Ortiz, J. V.; Baboul, A. G.; Stefanov, B. B.; Liu, G.; Liashenko, A.; Piskorz, P.; Komaromi, I.; Gomperts, R.; Martin, R. L.; Fox, D. J.; Keith, T.; Al-Laham, M. A.; Peng, C. Y.; Nanayakkara, A.; Gonzalez, C.; Challacombe, M.; Gill, P. M. W.; Johnson, B.; Chen, W.; Wong, M. W.; Andres, J. L.; Gonzalez, C.; Head-Gordon, M.; Replogle, E. S.; Pople, J. A. Gaussian 98, revision A.7, 1999. Gaussian Inc., 340 Quinnipiac St, Building 40, Wallingford, CT 06492.

(52) Frisch, M. J.; Trucks, G. W.; Schlegel, H. B.; Scuseria, G. E.; Robb, M. A.; Cheeseman, J. R.; Montgomery, J. A., Jr.; Vreven, T.; Kudin, K. N.; Burant, J. C.; Millam, J. M.; Iyengar, S. S.; Tomasi, J.; Barone, V.; Mennucci, B.; Cossi, M.; Scalmani, G.; Rega, N.; Petersson, G. A.; Nakatsuji, H.; Hada, M.; Ehara, M.; Toyota, K.; Fukuda, R.; Hasegawa, J.; Ishida, M.; Nakajima, T.; Honda, Y.; Kitao, O.; Nakai, H.; Klene, M.; Li, X.; Knox, J. E.; Hratchian, H. P.; Cross, J. B.; Bakken, V.; Adamo, C.; Jaramillo, J.; Gomperts, R.; Stratmann, R.

E.; Yazyev, O.; Austin, A. J.; Cammi, R.; Pomelli, C.; Ochterski, J. W.; Ayala, P. Y.; Morokuma, K.; Voth, G. A.; Salvador, P.; Dannenberg, J. J.; Zakrzewski, V. G.; Dapprich, S.; Daniels, A. D.; Strain, M. C.; Farkas, O.; Malick, D. K.; Rabuck, A. D.; Raghavachari, K.; Foresman, J. B.; Ortiz, J. V.; Cui, Q.; Baboul, A. G.; Clifford, S.; Cioslowski, J.; Stefanov, B. B.; Liu, G.; Liashenko, A.; Piskorz, P.; Komaromi, I.; Martin, R. L.; Fox, D. J.; Keith, T.; Al-Laham, M. A.; Peng, C. Y.; Nanayakkara, A.; Challacombe, M.; Gill, P. M. W.; Johnson, B.; Chen, W.; Wong, M. W.; Gonzalez, C.; Pople, J. A. Gaussian 03, revision C.02, 2004. Gaussian Inc., 340 Quinnipiac St, Building 40, Wallingford, CT 06492.

(53) Frisch, M. J.; Head-Gordon, M.; Pople, J. A. Semi-direct algorithms for the MP2 energy and gradient. *Chem. Phys. Lett.* **1990**, *166*, 281−289.

JM050624L